3 Soap bubbles and thin films

But all bubbles have a way of bursting or being inflated in the end.
Barry Gibbs, http://www.brainyquote.com/quotes/barrygibb199084.html

3.1 Introduction and early studies

Surfactants such as soap (sodium and potassium salts of fatty acids) stabilize thin liquid films, which are the basic structural units of foams and act as cell walls encapsulating the gas. The films are stabilized by surfactant monolayers of polar head groups (hydrophilic) solubilized in the water phase and aliphatic hydrocarbon tails (hydrophobic) protruding into the vapor phase. Isolated soap films can be easily produced by dipping a wire loop or rectangular frame into a soap solution and raising the frame slowly, causing the liquid to drain vertically. As the thickness of the film decreases from the top to the bottom of the frame, a pattern of interference fringes rapidly develops. This phenomenon can be spectacular, since each color band flows downward and a swirling motion is frequently observed due to rapid, complex fluid motion. Finally, toward the end of the thinning process, the film reaches a thickness that is less than the wavelength of light, and at this point, *black spots* appear, which spread rapidly, and eventually the entire film appears black in reflected light.

Foams, bubbles and foam films have been the subject of intense scientific investigations over a period of several hundred years. In the 17th century, both Robert Hooke (1) and later Isaac Newton (2) became captivated by these systems and carried out many fundamental experiments involving film drainage in bubbles in which the brilliant interference colors were carefully observed and reported in the *Proceedings of the Royal Society*. In Fig. 3.1, a typical spectrum generated by the drainage of thin foam films is illustrated.

It was also noted by scientists such as Newton and Hooke that, as the colored interference bands transformed to thin black films, the thinning ceased and eventually the films collapsed. This can be explained by the formation of a metastable state, resulting from the interaction of intermolecular forces. At first sight, the appearance of black spots was extremely puzzling. Hooke first thought that these black spots were black holes in the soap bubbles, and Isaac Newton, in his second paper on light and color, described (as illustrated below) the occurrence of several different states of thickness of

Fig. 3.1 Top: Isaac Newton and Robert Hooke. In addition to studies on gravity and the refraction of light from prisms, Newton studied the reflection of light from bubbles. Bottom: Brilliant interference colors resulting from the drainage of thin soap films. As drainage proceeds, the film thickness decreases from the upper to the lower region, and the color of the light changes according to the thickness of film. The swirling spectrum patterns observed on the surface are due to turbulence in the film causing regions of different thicknesses.

thin black films on bubble surfaces (as indicated by different shades of black and also the coalescence of the spots). According to Newton:

If a bubble be blown with water, first made tenacious by dissolving a little soap in it, it is a common observation, that after a while it will appear tinged with a great variety of colours. Besides the aforesaid coloured rings, there would often appear small spots of colours ascending and descending up and down the side of the bubble, the reason of some inequalities in the subsiding of the water; the sometimes small black spots generated at the sides, would ascend up to the larger black spots at the top of the bubble, and unite with it. (Isaac Newton`s Second Paper on Light and Color Proceedings of the Royal Society of London, 1675)

Following the early studies, it was almost 200 years later that major advances in foam structures were made by the Belgium physicist J.A.F. Plateau (3). In a classic text of 1873, Plateau derived the physical principles that determine the equilibrium geometry of polyhedral thin foam film structures. Toward the end of the late 19th century, C.V. Boys presented a series of lectures in 1889 at the London Institute; these lectures were reprinted in 1959 in a short publication (4), describing experiments with thin films (which were prepared using tinned iron wire frames), soap bubbles, water jets and fountains. In more recent times, several popular texts have been published on soap films, bubbles and foams, such as *Fizzics: The Science of Bubbles, Droplets, and Foams* by Young in 2011 (5) and *The Universal Foam: The Story of Bubbles from Cappuccino to the Cosmos* by Perkowitz in 2000 (6). In 2008, Seychelles and coworkers (7a and b) at the University of Bordeaux used the swirling colors created by

the flow of liquid on the membrane of a soap bubble to reproduce the curvature of the earth's atmosphere. Based on the modeling method, the strength and magnitude of typhoons, cyclones and hurricanes could be predicted. Patterns were also produced that mimicked the famous Great Red Spot on Jupiter. The spinning flow of liquid on the surface membrane of a soap bubble can be used to predict the strength of typhoons and to model cyclones.

3.2 20th-century studies on thin liquid films

Due to the complexity of foam systems, most attempts to study the fundamental mechanism of foaming have been carried out using simple models. These have been used fairly extensively; for example, the drainage and stability of a single soap film suspended on a vertical wire frame (pulled out of a bath of liquid) have been used to mimic the basic cell wall. Numerous other studies have been carried out with horizontal thin films, since this avoids the complications caused by the direct influence of gravitational forces. The experimental techniques used in these studies have been extensively documented. Unfortunately, most of these models are more useful from a fundamental viewpoint and have restricted applicability to real foam stability, since, although drainage is dependent on the characteristics of the film, it may occur as in planar or dimpled planar film or in a spherical direction or symmetrically or asymmetrically (Fig. 3.2). Nevertheless, it can be argued, for example, that the drainage and rupture of a single thin film in a foam system can lead to the destruction of an adjacent film. This can cause local fluctuations in pressure and surface tension, and thus this can lead to a collective effect. Generally, it has been established that the same factors which play a role in foam stability

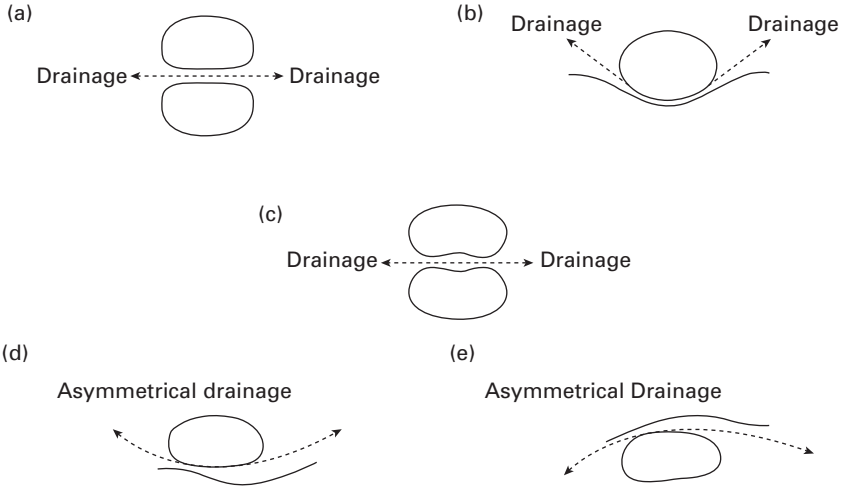

Fig 3.2 Drainage from different types of thin films: (a) planar film, (b) spherical film, (c) dimpled film, (d) and (e) asymmetrical films.

(film thickness, elasticity, etc.) appear to also have a decisive influence on the stability of isolated soap films. Hence, experiments with model films are very important.

However, it is obvious that real foams are much more complex, consisting of many inter-relating elements (Plateau–Gibbs borders and junctions). In fact, it is crucial to consider the role of the Plateau borders under both dynamic and static conditions, since all stresses on foam films are transmitted through the Plateau borders. In the following sections, the drainage of model foam systems will be discussed in some detail. In order to study the fundamentals of foams and foaming it is important to understand the behavior of self-supporting thin films where gravity is the main driving force that causes draining and instability. For non-horizontal films, gravity acts directly, but in the case of horizontal films it acts indirectly through suction of the Plateau borders.

3.3 Experimental techniques for investigating free horizontal circular liquid films

Over the past half a century, extensive studies have been carried out to quantify the thinning and stability mechanisms in terms of interfacial interactions of small, free microscopic horizontal foam films. Experiments have been carried out utilizing different types of specialized thin film equipment which operates by maintaining a balance between the forces within the thin film and an applied external gas pressure and the bulk liquid pressure in the Plateau borders. Most quantitative studies on film drainage have been carried out using a micro-interferometry technique to observe and measure the changes in thickness (drainage) of horizontal foam films, and this is described in the following section. Initial studies were made with small, horizontal circular films in the size range of 0.05–1.0 mm which were formed from a concave liquid drop suspended in a short vertical capillary tube using adaptations of the techniques pioneered by Scheludko and coworkers (8, 9, 10). Further developments led to the design of a porous plate (11) and a bike wheel thin film apparatus (12, 13) which enabled isotherms (directly relating disjoining pressure to film thickness) to be accurately measured. Such experiments enabled the intermolecular forces and dispersion force contribution to the disjoining pressure to be evaluated.

3.3.1 The conventional Scheludko/Exerowa thin film balance

This method was originally developed and described by Scheludko and improved by Exerowa and other Bulgarian research workers (11). From these studies, important advances have been made in thin film research, enabling the basic physical/chemical nature of the stability and thinning process to be understood. A diagram of the experimental equipment is presented in Fig. 3.3.

To begin the experiment, a film is formed between the tips of the menisci of a biconcave drop held in a cylindrical glass film holder (of about 2 mm radius) which is fused to a capillary tube with an access port for withdrawal of excess liquid. The film is produced by sucking a solution containing a defined quantity of surfactant through

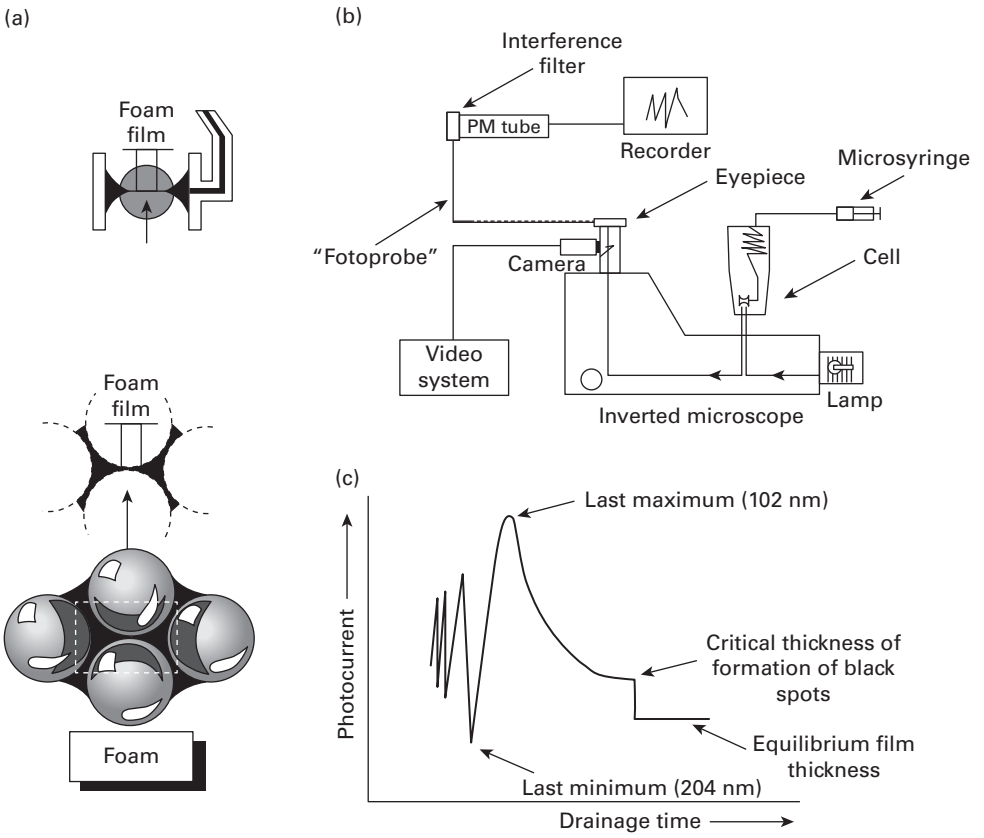

Fig. 3.3 Schematic representation of the instrumentation for studying thin horizontal liquid films. The film is formed between the tips of the meniscus of a biconcave drop held in a glass cell as illustrated. From ref (11).

a tube, as illustrated in Fig. 3.3(a). The amount of liquid in the biconcave drop is controlled by a micro-syringe, which enables the radius of the film to be varied. The measuring cell (containing the glass-tube holder of the film) is enclosed in a water jacket which is maintained at a constant temperature. The cell is positioned on the stage of a metallographic microscope (Fig. 3.3b). Light from a quartz-halogen source passing through a monochromatic interference filter (wavelength = 546 nm) is incident on the film surface. The light signal, which is reflected from a small portion of the film, is directed onto a photo-detector, converted into an electric signal, amplified and finally recorded. The film is also observed in reflected light through a calibrated eyepiece, and the radius of the film is determined visually.

Precautions are taken to eliminate the effect of external disturbances, such as vibrations, on the film thinning process. The film thickness (h) at any instant of time is estimated from the intensity of the photocurrent, which is related to the refractive index of the solution and the wavelength of the monochromatic light. The maximum and minimum intensities of the photocurrent are recorded until the last maximum is reached

and finally an equilibrium thickness is established (Fig. 3.3c). Corrections to the film thickness and also a correction to account for the differences in optical density of the adsorbed surfactant layers which differ in refractive index from water and the aqueous core are made. The real film thickness is derived from an equation that also takes into account the thickness of the layer formed by the hydrocarbon tails of the surfactant molecules adsorbed on the film surface.

3.3.2 The porous plug film holder to measure disjoining isotherms and surface forces in thin films

With the conventional Scheludko/Exerowa film holder described in Section 3.3.1, the maximum pressure attainable is relatively low (300 to 400 Pa), and this limits the range of disjoining pressures which can be investigated. In order to overcome this problem, a porous plate thin film holder was developed, which is shown in Fig. 3.4.

This technique enabled isotherms (directly relating disjoining pressure to film thickness) to be determined at higher pressures. The porous plug plate is constructed by drilling a hole through a fritted disk which is fused to a capillary tube. The maximum capillary pressure attained was much higher than the conventional Scheludko/Exerowa cell due to the small size of the pores (about 4 microns) through which the solution is drained. Single films are formed in the film holder, which is enclosed in a sealed plexiglass cell with the capillary tube exposed to a steel chamber.

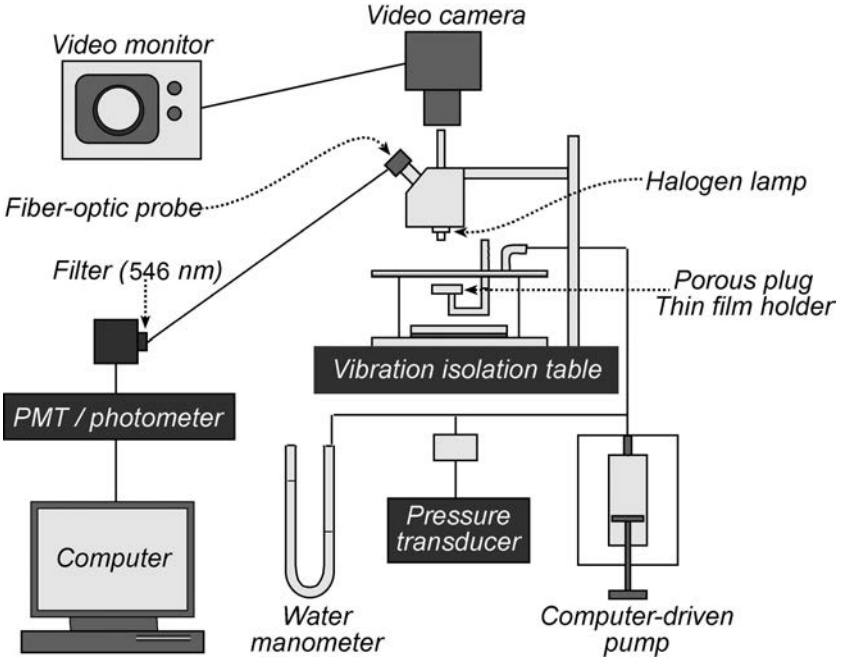

Fig. 3.4 Modified experiment with porous plug and video camera. From ref (11).

Manipulation of the pressure inside the cell enables the pressure on the film and therefore the disjoining pressure to be adjusted, and the pressure in the cell is regulated by a computer-controlled syringe. After establishing equilibrium conditions, the film thickness is measured interferometrically and the disjoining pressure is calculated from the pressure balance between the applied gas pressure and the bulk liquid pressure in the Plateau borders. A digital video camera is mounted on the microscope which enables visual inspection of the film to be carried out. The only disadvantage reported with the porous silica plate holder was that it had a high negatively charged internal surface area on which positively charged cationic surfactant can adsorb reducing the bulk concentration.

3.3.3 The bike wheel microcell film holder

Further developments in cell design lead to the bike wheel microcell film holder (Fig. 3.5) developed by Cascao-Periera and coworkers (12, 13) and which was modified from the conventional capillary-type holder. In this cell, the dimension of the capillary into which the film is formed was considerably reduced (about tenfold).

An additional advantage of this cell holder is that it does not operate by side drainage as in conventional cells, and it also has a lower exposed surface area. Dimple formation or bowing of the fluid interface due to pressure gradients can also be avoided using this film holder, and less time is required in draining to reach an equilibrium film with plane parallel interfaces. In this cell, the capillary pressures attained are comparable to those obtained with the porous plug holders but the sizes of the films are nearer to the sizes encountered in real foams systems. The small channels

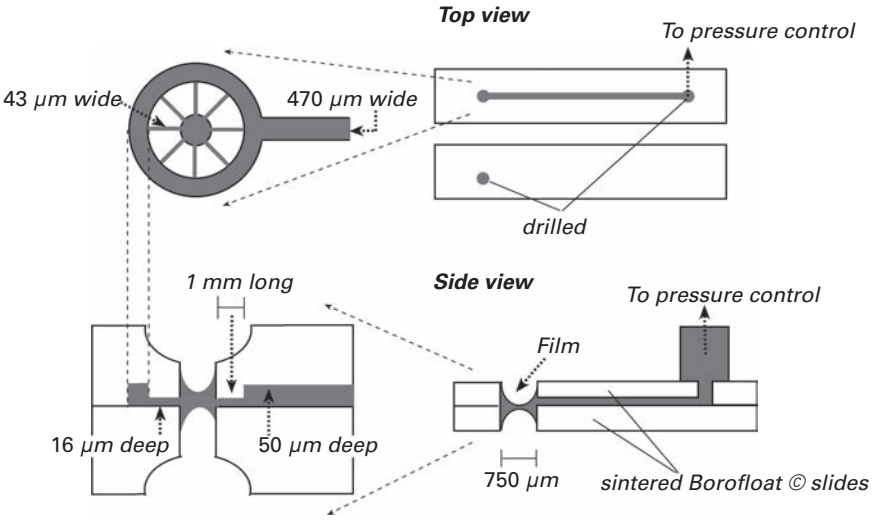

Fig. 3.5 Schematics of the bike wheel chip of the film holder. For clarity only 8 of the 24 thin drainage channels are shown. The channels connect the small orifice with the thin film which is formed in the annulus. From ref (12).

were manufactured using micro-fabrication techniques encountered in the semiconductor industry. The cell holder is constructed by sintering two plates wherein one of them contains a micro-machined pattern, and this produces orifices and channels which are enclosed between them. The orifices are drilled through both sides and serve as capillary tubes where the films are formed and are tapered on the outside to constrain film formation at the center-line. A second orifice is situated in the upper plate which serves as an opening. A horizontal channel connects the annulus, where the film is formed, to the second orifice on the upper plate and allows for the continuous flow of solution and drainage. The first orifice, where the film is formed, is connected by 24 pores to the annulus, and these pores are distributed around the orifice, producing a bike wheel pattern.

3.3.4 The Nikolov/Wasan film balance for measuring drainage and film thickness of curved foam films

In addition to flat horizontal thin films, experiments on curved films have been successfully carried out by Sethumadhavan and coworkers (14) using the cell shown in Fig. 3.6. An air bubble is formed from a small capillary (about 0.5 mm radius) and the solution level around the bubble is lowered until the film size is of the required dimension. Using a reflected light interference microscope, the white light from the top incident on the film surface is reflected from the top surface of the film, thus producing interference patterns. The use of a microscope, a CCD camera and image analyzer enables the interference patterns as a function of time to be monitored and hence also the drainage rate. The size of the bubble affects the capillary pressure, which is kept constant by monitoring the pressure using a pressure inducer. Using this type of film balance, studies were carried out with thin liquid films containing monodispersed colloidal particles.

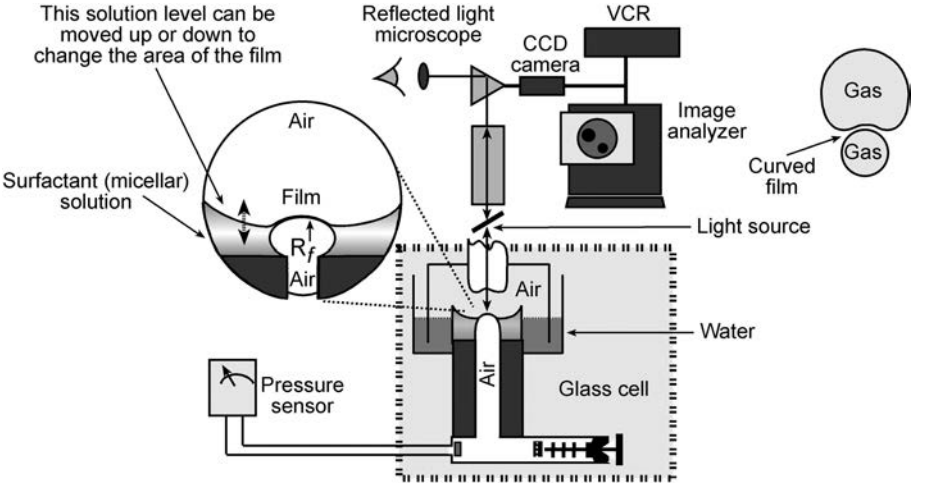

Fig. 3.6 Film balance used for measuring film thickness and drainage of curved foam films. From ref (14).

3.4 Drainage of horizontal thin films

Direct measurement of the change in thickness of the aqueous film can be determined by micro-reflectance methods. In addition, the drainage time can be recorded so that *the drainage rate (velocity of thinning)* can be compared with the theoretical value for a flat film calculated using the Stefan–Reynolds equation (15)

$$T_{\mathrm{d}} = \int_{h_{\mathrm{t}}}^{h_{\mathrm{i}}} \frac{dh}{V} \tag{3.1}$$

where T_{d} is the time of drainage of the film, h_{i} is the initial thickness and h_{t} is the final thickness after drainage. Also, $V_{\mathrm{d}} = -dh/dt$ represents the velocity of thinning and t is the time of thinning. For the above equation, in the case of horizontal, fairly thick films (>100 nm), Scheludko (8) modified the Stefan–Reynolds equation and derived an expression for the thinning rate between two disc surfaces $(V_{\mathrm{R_e}})$ under the influence of a uniform external pressure. The change in film thickness with drainage time can be expressed as

$$V_{\mathrm{R_e}} = -\frac{dh}{dt} = \frac{2\Delta P h^3}{3\eta_\ell R_f^2} \tag{3.2}$$

where R_f is the radius of the disc, η_ℓ is the viscosity of the liquid and ΔP is the pressure difference between the film and the bulk solution and is equivalent to the capillary suction P_{c} in the Plateau border. For very thin films, the pressure gradient also includes the disjoining pressure. The main conditions for the applicability of Equation (3.2) are (a) the liquid flows between plane parallel surfaces; (b) the film surfaces are tangentially immobile; and (c) the rate of thinning due to evaporation is negligible in comparison with the rate of thinning due to drainage.

Early experimental studies carried out in the 1950s and 1960s by Scheludko's group (8, 9) with comparatively thick rigid films produced from dilute sodium oleate and isoamyl alcohol surfactants in dilute electrolyte were in reasonable agreement with the drainage equation. In such cases, wall effects caused by the mobility of the surfactant adsorbed layers (surface transportation) were almost eliminated. However, for most systems, enhanced deviations from the Reynolds equation occur due to tangential surface mobility. Strictly speaking, tangential surface mobility can never be completely eliminated in foam films with soluble surfactants. The concentration gradient caused by the outflow of surfactant (and also the surface tension gradient which slows down or prevents flow in the surface) is partially compensated by the surfactant diffusion from the bulk film (diffusion relaxation). This relaxes the effect due to the surface tension gradient and produces a state of slip at the interface, thus causing an increased drainage rate compared to the Reynolds model. In addition, surface viscosity can also slow down the drainage. The overall situation describing the drainage of films is summarized in Fig. 3.7, where the mobility of the interface, the surface tension gradients and the diffusion of surfactant molecules are all shown to have important roles in controlling the drainage rates.

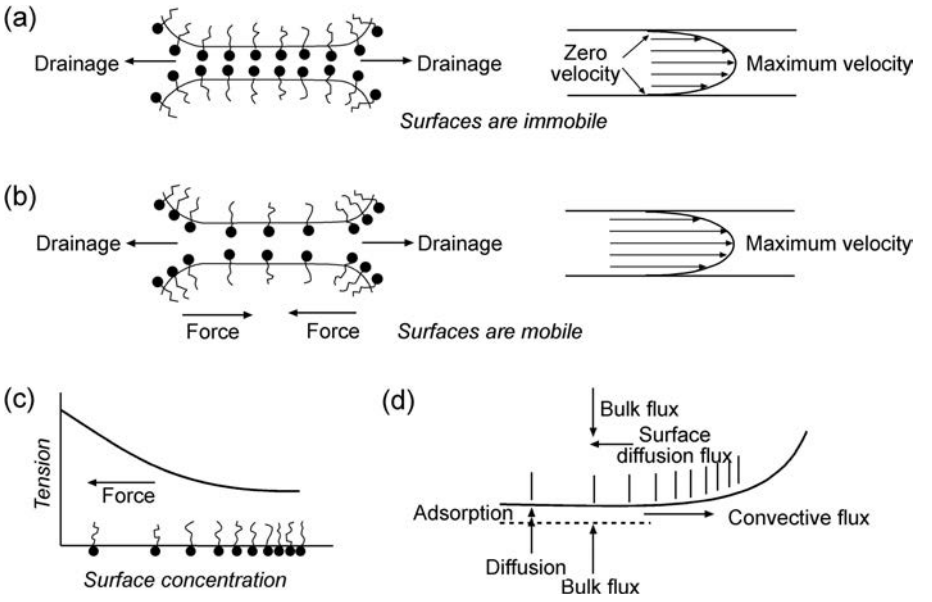

Fig. 3.7 (a) For thick films (> l00 nm) the drainage is dictated by the mobility of the interface. The drainage velocity $V_{Re} = -dh/dt$ can be determined from the Reynolds equation, which is valid for (a) an ideal circular film between two rigid plates pressed by an external force with an idealized rigid surface with zero tangential flow at the surface. (b) However, in the case of most surfactant films, the surfaces are not rigid and the tangential velocity at the surface is not zero. Surface mobility is $V > V_{Re}$ due to the concentration gradient caused by the outward flow of liquid. (c) The surface mobility during drainage causes interfacial tension gradients, and the surface tension varies with surface concentration. (d) This may also cause diffusion along the surface and from bulk solution with both adsorption and convective flow. This results in a surfactant mass balance at the film interface.

At high surface tension gradients and low surface mobility, the drainage is reduced and this usually becomes pronounced when the surfactant is present in the film at concentrations near the CMC, where the bulk diffusion coefficients are small and the Gibbs elasticity is large. Also, the adsorption and diffusion of surfactant from the bulk solution must be taken into consideration (Fig. 3.7d). Generally, for thinner films, large electrostatic repulsive interactions can reduce the driving force for drainage and may lead to stable films. Also for thick films containing high surfactant concentrations (> CMC), micelles in the film can cause a repulsive structural mechanism.

Also, the effect of deformation of the film surface during thinning is extremely complicated. In more recent years, the question of the profile has been under intense discussion, because when two drops approach, the film is not initially planar. Due to frictional resistance, liquid from the center part of the film flows out more slowly than the edges and this causes a *dimple* to form. The dimple consists of a central lens of entrapped fluid with a thicker peripheral ring (16, 17), and this can have a significant influence on the drainage. Frankel and Mysels (18) were the first researchers to put forward the hydrodynamic theory for the profile and evolution of the dimple. The rate of

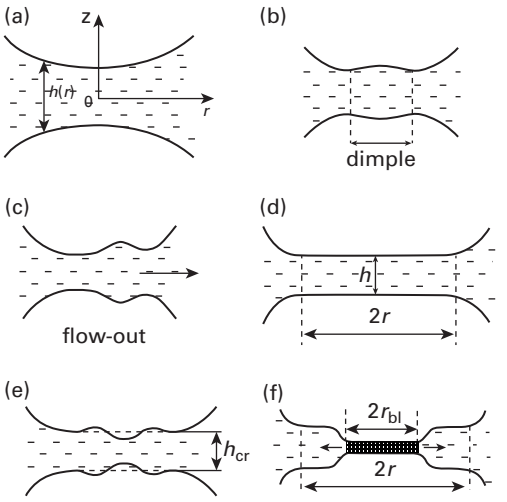

Fig. 3.8 Schematics of the basic stages of thinning of a liquid film captured between bubbles. (a) Approach of the non-deformed fluid, (b) a dimple is formed, (c) the flowing out of the dimple results in plane parallel film, (d) thinning of plane parallel film thickness h and radias r (e) when the transition thickness h_{cr} is reached a thin black spot results (f) the black spot radius $r_{b\ell}$ expanded radially until it occupies the whole area. From ref (19).

thinning at the ring barrier was shown to be higher than the rate of thinning at the center of the ring. A symmetric dimple will slow down thinning, but an asymmetric dimple can accelerate thinning. The next stage in the drainage process usually involves the disappearance of the dimple and the formation of the plane parallel film (to which the Stefan–Reynolds drainage equation is applicable). Finally, this is followed by the formation of a hole or thin spot which expands, leading to coalescence. At film radii below 0.1 mm, dimple formation is visually undetectable, as a rule, at any thickness. In Fig. 3.8 the various stages suggested for the thinning of a soap film involving the dimpling process are shown.

Drainage research over the past 40 years has been involved with quantifying the relevant parameters that determine if the film will drain rapidly (promoting instability) or slowly (due to resistance from the boundary layer). Joyce and coworkers (20, 21) developed a numerical model, and Malholtra and Wasan (22) modified the Reynolds model by accounting for the flow in the Plateau border as well as the effect of van der Waals forces. This approach led to a generalized model which accounts for the effect of the mobility of the surface on thinning by considering the kinetics of adsorption/desorption of surfactant, surface and bulk diffusion, surface rheological properties and flow (in both film and bulk phases).

Several other workers have developed hydrodynamic models of film drainage and taken into consideration the most influential properties such as surface tension gradients, surface shear, surface viscosities and dilational viscosities, etc. (23 to 25). Such treatments frequently involved the derivation of complex equations which require numerical integration. Sharma and Ruckenstein (26) suggested that surface oscillations (surface

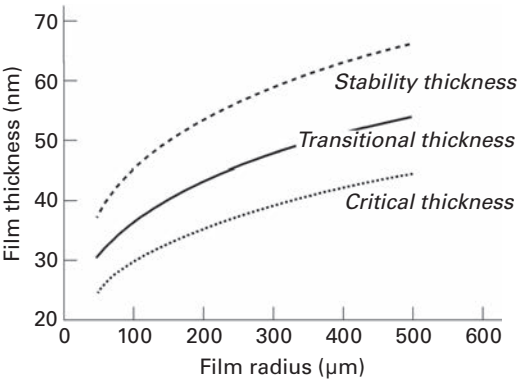

Fig. 3.9 The stability, transitional and critical thicknesses of foam films calculated from different models and comparison with experimental data in the literature. From ref (27).

waves) cause an outward flow of liquid, resulting in a pumping action from the center to the rim. A mathematical analysis of the situation was made by superimposing the Reynolds thinning process on this pumping action, giving an enhanced thinning velocity. However, even today, some of the basic hydrodynamics involved in the drainage of thin films are not clearly understood, and it is important to relate the tangential surface mobility to the size of the film.

Valkovska and coworkers (27) studied the partial mobile drainage of thin films with respect to axisymmetric interfacial fluctuations of the film and developed a model which included several relevant interfacial properties such as the Gibbs elasticity, the surface and the bulk diffusion, etc. Both radially bounded and unbounded interfacial fluctuational waves were taken into consideration, and three differing film thickness modes were identified corresponding to (a) a stability thickness h_{st}, due to the loss of stability of the film; (b) a transitional thickness h_{tr}, when waves which causes film rupture becomes unstable; and (c) a critical thickness h_{cr}, where the film finally ruptures. From their theory, film thickness values were calculated which were related to the film radii. Some of the results of the computations are shown in Fig. 3.9, which appeared to be in reasonable agreement with experimental data taken from the literature.

Manev and Nguyen (28) reviewed the literature on film drainage and commented that many of the theoretical studies did not take into account spatial variation and heterogeneity in film thickness. Experimental studies by Manev, Tsekov and Radoev (29) clearly established that non-homogeneities occur during film thinning (particularly with films with larger diameters), and in Fig. 3.10, a series of film profiles, recorded during the last stages of thinning, show a wide range of surface deformation and thickness heterogeneity that evolved over the surface of the film.

These workers proposed a model (known as the MTR theory) which included the effects of surface deformation and thickness heterogeneity (dimpling effects) on drainage (29). In theory, the energetic sources of the dimpling (or surface corrugation) and the outflow of liquid from the film were taken into consideration. In many early

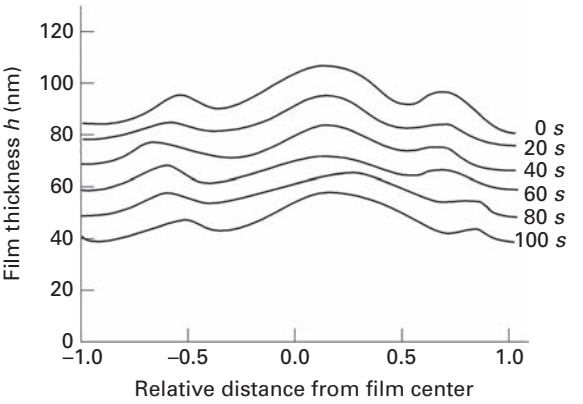

Fig. 3.10 Evolution of the film profile during the last stages of thinning for a solution of sodium dodecylsulfate (1.0 mmol/l) + KCl (0.1 mol/l). The radius of the film was r = 1.0 mm and the amplitude of the thickness heterogeneity was ca 25 nm. The time intervals indicated from 0 to 100 s is counted from an arbitrary initial film thickness (h). From ref (28).

theories, only relatively small amplitude thermal corrugations were used to explain the scale of corrugation, whereas in the MTR model, a description of the non-homogeneity of the film thickness was derived by dividing the total film surface into several thinner decay domains, and it was also assumed that the film disintegrated into an ensemble consisting of several smaller centers. According to this theory, the amplitude of the thickness heterogeneity increased with film radii, so that films with large radii can be visualized as consisting of many small individual films which under favorable hydrodynamic regimes drain more rapidly (causing accelerated drainage). From this theory, the rate of thinning could be expressed by the equation

$$V_{\mathrm{d}} = \left(\frac{1}{6\eta_{\ell}}\right)\left(\frac{h^{1/2}\Delta P^{8}}{4\gamma^{3}r_{t}^{4}}\right)^{1/5} \tag{3.3}$$

where V_{d} is the velocity of drainage or thinning, γ the surface tension of the liquid, r_{t} is the film radius, h is the film thickness, and ΔP is the driving pressure or the difference in capillary pressure and disjoining pressure. This theoretical model gave improved agreement with experimental drainage data for small and large horizontal thin films.

3.5 Drainage of vertical thin films

Foam films can also be produced by pulling a vertical frame out of a reservoir solution. The characteristics of the film can be studied in three stages: (a) the initial formation of the film, as defined by its starting thickness, which is determined by the withdrawal velocity; (b) the drainage of the liquid within the lamella, which causes thinning with time; and (c) the aging of the film, which may lead to a metastable state. At first sight, it may appear that the main mechanism in (b) that causes the gradual descent of liquid is

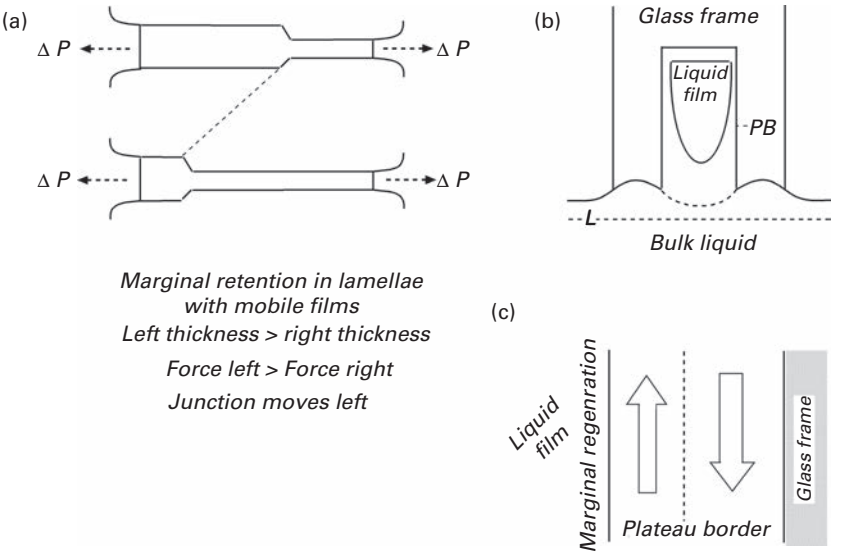

Fig. 3.11 Marginal regeneration. (a) The thicker film is drawn into the border by the excess pressure ΔP and the thinner film is pulled out of the border. (b) Schematic view of film, and (c) close-up of flows in Plateau border of a vertical film. Two flow regions are indicated; in the film-near region, the liquid flows upward while near the frame the liquid flows downward. From ref (30).

gravitational drainage. This drainage, when expressed as an average velocity (V_{av}), can be described by the viscous flow of liquid (under gravity) between parallel plates:

$$V_{av} = \frac{\rho_\ell g h^2}{8\eta_\ell} \tag{3.4}$$

where h is the film thickness, ρ_ℓ is the density of liquid in the film, η_ℓ is the bulk viscosity of the liquid and g is the constant of gravitational acceleration.

Again, as in the case for horizontal films, it may be assumed that the monolayer of surfactant at the boundaries of the film is rigid (i.e. no-slip boundary conditions). However, this vertical drainage mechanism is only important for fairly thick films. In fact, as the process proceeds, the thinning can also occur by a horizontal mechanism known as "marginal regeneration," in which the liquid is drained from the film near the border regions and exchanged with liquid from within the low-pressure Plateau border. In this exchange, the total area of the film does not change significantly. Also, since the liquid can only be drawn from the small thicker region adjacent to the border, this region is reduced in thickness. It then acts as a constriction preventing any further flow of liquid (Fig. 3.11a).

This causes two films of different thickness to be formed in contact, with the border regions with the thicker film having the greater force, drawing solution into the border and resulting in the formation of patches of thin film at the border, with the excess liquid flowing into the border channel. Overall, the edge effect determines drainage, with the general rate of thinning varying inversely with the film width. The phenomenon was

originally described in early pre-2000 by thickness fluctuations caused by capillary waves. The drawing mechanism, continuously occurring at adjacent regions of the border, can lead to rupture, originating at the margin.

Marginal regeneration is not well understood, but it is probably the most important cause of drainage in vertical thin liquid films with mobile surfaces. This situation is frequently encountered in foams containing surfactant solutions at concentrations above the CMC. Stein and coworkers (30, 31, 32) have carried out many detailed experiments on this subject in which the surface flow and bulk flow of liquid (caused by the pressure gradient) were analyzed. The flow in the Plateau border was detected by the addition of small glass beads into the system, as illustrated in Fig. 3.10b. One of the problems involves the determination of the local pressure in the Plateau border connecting the vertical thin film with the supporting frame. The difference in marginal regeneration at the top, bottom and vertical side Plateau borders in a vertical film was explained by surface waves causing a squeezing mode (32).

Several post-2000 theoretical models have been proposed to account for the experimental drainage data. Naire and coworkers (33) derived three coupled nonlinear partial differential equations which described the influence of film shape, surface viscosity and surfactant transport for the case of insoluble monolayer on viscous incompressible vertical free liquid film. These workers examined the case where film was nearly flat, so that mean surface tension was negligible, and verified that increasing surface viscosity slows down drainage, enhancing the stability of the film. However, in their case studied, it was also found that the Marangoni effect, which reduced drainage, had only a weak influence on drainage. Braun and coworkers (34) derived nonlinear partial differential equations based on lubrication theory to model the drainage of vertical films which contained insoluble surfactant. In this case, the effects from gravity, viscosity, surface tension and its dependence on surface concentration (the Marangoni effect) and surface viscosity were included in the derivation. The models were able to predict very fast and slow limits of drainage, which had been observed experimentally, and also a limited range of intermediate drainage rates. For low surface viscosities, a transition from a mobile to an immobile film was predicted for increasing surface tension gradients, and this has been observed in practice, for example in dip coating processes in the presence of insoluble surfactant.

Berg and coworkers (35) experimentally determined the thickness of freely suspended surfactant films during vertical withdrawal and drainage processes using a laser reflectivity method. Films were prepared with SDS surfactant, and glycerol was added to some of the solution at concentrations above the CMC to extend the lifetime and reduce evaporation. Initial film thicknesses were found to be in the micrometer range, and it was suggested that subsequent thinning was mainly impelled by capillary rather than gravitational forces. It was also found that thinning above and below the CMC could be approximated by a power law function in time. However, the experimental results were found to be generally inconsistent with the current description of capillary–viscous drainage in inextensible films, and it was concluded from the study that a significant amount of drainage flux induced by Marangoni flow occurs above and below CMC and it was important to consider these flow instabilities along the film

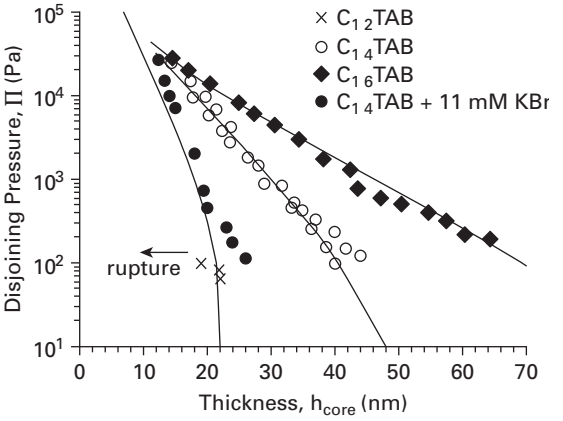

Fig. 3.12 Disjoining pressure versus film thickness for various CnTAB foam films. In all cases the surfactant concentration is equal to the salt-free CMC of the surfactants, and the curves represent constant charge DLVO fits to the data. From ref (36).

borders (marginal regeneration effects) in modeling vertical drainage for both entrained and draining films. Conventional hydrodynamic models of soap films in which non-slip conditions were widely used were considered to be inadequate, and it was necessary to include in vertical film drainage, the influence of the adsorption/desorption of surfactant and to introduce an interfacial slip parameter.

3.6 Disjoining pressure isotherms obtained from porous plug experiments

Bergeron (36) carried out a systematic study with a series of alkyltrimethylammonium bromide surfactants (CnTABr) with different chain lengths. Disjoining pressure isotherms (directly relating disjoining pressure to film thickness) were determined using the porous plug film holder. These data were collected under relatively low pressures, and the results are shown in Fig. 3.12. These curves show that, on increasing the surfactant chain length, the repulsive force is increased (in the order $C_{16} > C_{14} > C_{12}$) as the film thickness is reduced. In all cases, fairly thick equilibrium common black films (CBFs) were formed (70–15 nm). Also, with n =12, a lower rupture pressure was obtained in comparison with the longer chain surfactants, although the stability of this shorter chain length surfactant was found to increase with the addition of a low concentration of electrolyte (KBr).

3.7 Intermolecular forces are the reason that thin films are stable

Scheludko (9, 10, 11) also found that for thin films (< 100 nm) the rate of drainage began to deviate from that predicted from Equation (3.2), and during the final stages of thinning, surface forces come into play. In the 1950s, Derjaguin and Titievskaya (37) proposed that this mechanism could be explained by a positive (repulsive) disjoining

pressure which slows down and prevents the drainage process. In addition to the Laplace capillary pressure, two additional types of intermolecular forces can operate in aqueous film layers at low surfactant concentrations (<CMC): (a) the electrostatic double layer repulsion Π_e and (b) the van der Waals Π_{vdw} interactions. The Derjaguin's disjoining pressure Π includes these two contributions as shown in the equation

$$\Pi = \Pi_{el} + \Pi_{vdw} \tag{3.5}$$

From well-known DLVO theory (38) Π can be expressed in terms of the dispersion and electrostatic components as

$$\Pi(h) = \frac{64nkT}{k}\gamma^2 \exp(-\kappa h) - \frac{A_H}{12\pi h^2} \tag{3.6}$$

where

$$\gamma = \frac{\exp(Z/2) - 1}{\exp(Z/2) + 1}, \quad Z = \frac{e\psi_0}{kT} \tag{3.7}$$

and A_H is known as the Hamaker constant, n^0 is the number density of ions in the bulk solution, k is the Boltzmann constant, T is the temperature, κ is the inverse Debye length, e is the electron charge, ψ_0 is the potential, and Z is the valency. The weak-overlap approximation is used here for the electrostatic contribution.

Thin film stability is achieved when the disjoining pressure is repulsive; the film then resists thinning and rupture caused by small perturbations. At equilibrium and in the flat portion of the film, the disjoining pressure Π is equal to the imposed capillary pressure P_C. The latter is simply the difference between the gas pressure, P_g, and the bulk liquid pressure, P_ℓ, in the Plateau border region surrounding the film. In regions of low electrolyte concentration the drainage proceeds and Π_e dominates over Π_{vdw}, but eventually an equilibrium is established between the electrostatic repulsive interaction and the capillary pressure; that is, $\Pi_{el} = P_c$.This results in the formation of an equilibrium-free film that is usually referred to as a thick common film *CF*, which is about 50 nm thick. This type of film reaches a state of equilibrium which persists until thermal or mechanical fluctuations cause rupture. In addition, from Equations (3.5), (3.6) and (3.7), the interfacial potential may be calculated from the thickness of the films. In practice, the critical thickness value at which this common film may rupture (due to thickness perturbations) has been designated h_{cr}, and since the process of rupture is statistical, experimental observations of the thickness of rupture always show a distribution at, or near, h_{cr}.

However, at high electrolyte concentration, the thick common film cannot achieve stability and on reaching h_{cr} the film thins further and undergoes a further first-order transition, finally leading to a stable thin black film (otherwise known as a Newton black film, Perrin film or secondary black film) which is usually about 4 nm thick. The surfactant concentration associated with the onset of thin black film formation is critical, as it indicates a phase transition of the surfactant monolayer, due to high packing

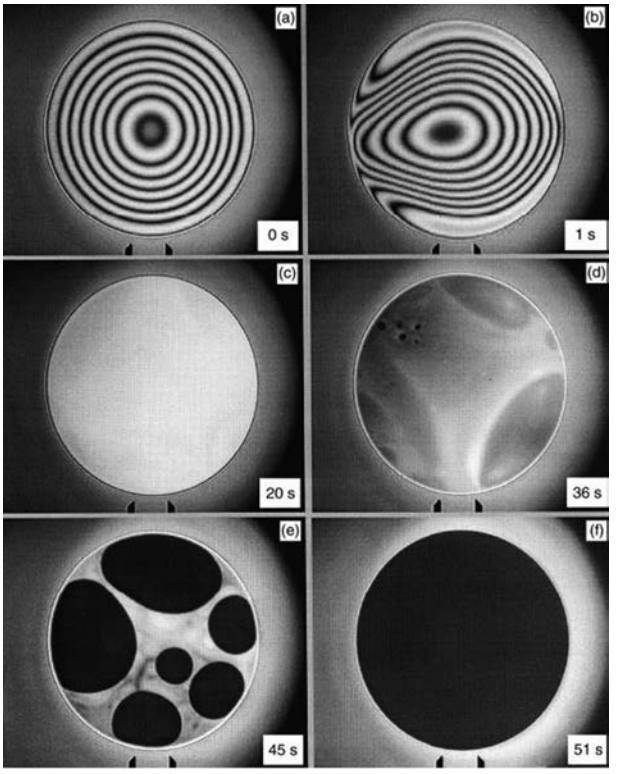

Fig. 3.13 Typical interference patterns of the thinning of a foam film containing sodium dodecyl sulfate (2×10^{-4} M): (a) a dimple between the film surface; (b) flow-out of the dimple; (c) thinning plane parallel film; (d) appearance of the first black spots; (e) enlargement of the spots; (f) final stable black film. The time elapsed from the moment of the film formation is indicated in the lower right corner of each picture. The film diameter is 220 microns. From ref (39).

density and the onset of charge reduction. Such a phase change is the determining factor of the stability of the thin film. This idea that such a phenomenon is due to a change of state of the surfactant was originally proposed by Scheludko and coworkers (9). Such a change probably involves condensation of the adsorbed surfactant layer from gaseous to an expanded liquid state. The interference patterns of the different steps in the thinning process are illustrated in Fig. 3.13.

The formation of this metastable film can be experimentally observed through the formation of "islands of spots" which appear black in light reflected from the surface. The spots are sometimes referred to as holes in order to emphasize the thinner regions in the film, and the holes spread over the complete film surface. This is often considered to be the "first black" film as originally described by Hooke (1), or the "common black film." The lowest bulk surfactant concentration at which nuclei of the thinner black films are formed has been designated "c-black" (c_b), and it has also been shown that the black films and spots can coexist in patches with ranges of thickness, and stepwise transitions can occur between regions.

This causes changes in the rheological properties of the adsorbed film and it becomes resilient to rupture with low gas transfer. Black spots usually appear at a surfactant concentration above which the foam becomes extremely stable with a lifetime greater than 10 mins. Highly persistent bubbles and foams have been produced and shown to depend on the type of surfactant and concentration is usually one order of magnitude higher for ionic surfactants compared to nonionics.

The exposure and characterization of two types of black films has been one of the most significant advances in foam film experimentation, and to explain the stability of the secondary black film, it was found necessary to include an additional short-range hydration or structural repulsive force defined as Π_{st}, which is caused by steric hindrance from the orientation of the tightly packed surfactant molecules at the liquid/vapor interface which increases the stability and must be considered in the overall interaction. Therefore, the disjoining pressure versus film thickness isotherms were modified to include this short-range repulsion and redefined as

$$\Pi = \Pi_{el} + \Pi_{vdw} + \Pi_{st} \tag{3.8}$$

De Vries (40) was one of the first researchers to stress the relevance of the van der Waals forces in foam films and suggested that the common black films corresponded to a secondary minimum in the potential energy versus separation distance. The stability (which prevents further thinning) of the NBF is determined by the short-range repulsive disjoining pressure caused by the thin bilayer structures with a few molecules of water separating the two opposing monolayers. The critical electrolyte concentration C_{crit} corresponding to the transition from common thin films, (CTFs) and common black films (CBFs) to NBFs is also an important feature of these film thinning studies; it has been shown to depend on the type of surfactant and is usually one order of magnitude greater for ionic compared to nonionic surfactants. In Fig. 3.14, the Π versus h isotherm is shown, which can be conveniently used to explain equilibrium conditions and transitions from common black films (CF_s) to NBFs, with the two stable (equilibrium) thicknesses corresponding to a given disjoining pressure indicated.

The conditions of equilibrium of the common films, CBFs and the transition from CBFs to NBFs have attracted a great deal of attention over the past 30 years. The thickness of the film is strongly dependent on the ionic strength of the liquid, and the stability of the film is dependent on the maximum height of the primary potential energy barrier. This is illustrated in the potential energy versus film thickness plot which is derived from DLVO theory. In cases where the film thins further and overcomes the primary maximum potential energy peak, it will fall into the primary minimum potential energy sink, where very thin Newton films are formed.

In the case of nonionic surfactants, experimental foam film studies carried out with aqueous solutions of poly(ethylene oxide), $C_{10}(EO)_{12}$ and $C_{12}(EO)_5$, the equilibrium thicknesses of the foam film was related to the surfactant concentrations, as shown in Fig. 3.15, and the surface potential of the interfaces was also calculated from DLVO theory (41). Similar film thickness and surface potential values were obtained from experiments carried out using low concentrations of surfactants with different chain

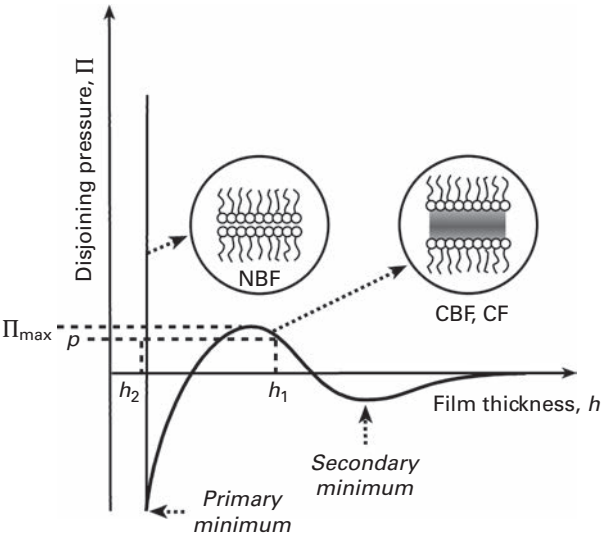

Fig. 3.14 The general form of the force curves (disjoining pressure Π versus film thickness h) for a thin film containing fairly low concentrations of surfactant. P_c is the capillary pressure. h corresponds to a common film (CF) about 300 Å thick, h_1 to a common black film (CBF) and h_2 to a Newton black film (NBF) about 40 to 50 Å thick. The isotherm shape depends on the type and concentration of surfactant and electrolyte.

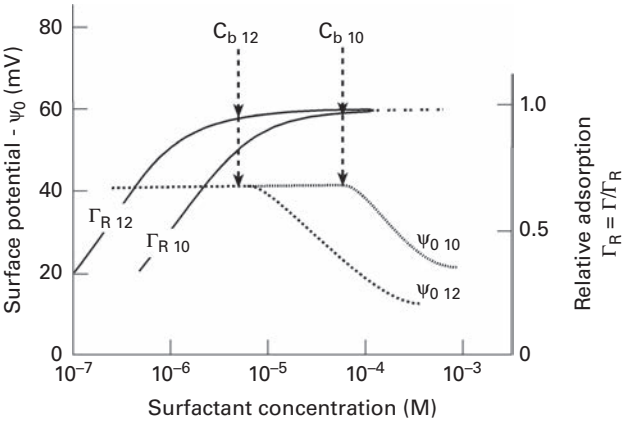

Fig. 3.15 Surface potential (ψ_0) and relative surface adsorption density (Γ_R) versus concentration of $C_{10}(EO)_5$ and $C_{12}(EO)_5$. The relative adsorption density $\Gamma_R = \Gamma/\Gamma_m$ where Γ is the surface excess of surfactant (determined from surface tension measurements) and Γ_m is the maximum amount of surfactant adsorbed at close packing. The figure shows that the onset of potential decrease corresponds to a high relative surface adsorption density for both systems. The C_b values, at which black spots appear in the aqueous films, are indicated. From ref (41).

lengths. A film thickness of about 60 Å (which is equivalent to a negative surface potential of about –40 mV) was measured which may be considered to be rather surprising for a nonionic surfactant considered to be nonpolar. However, similar behavior was earlier reported for soap films stabilized with amine oxide and sulfoxide nonionic

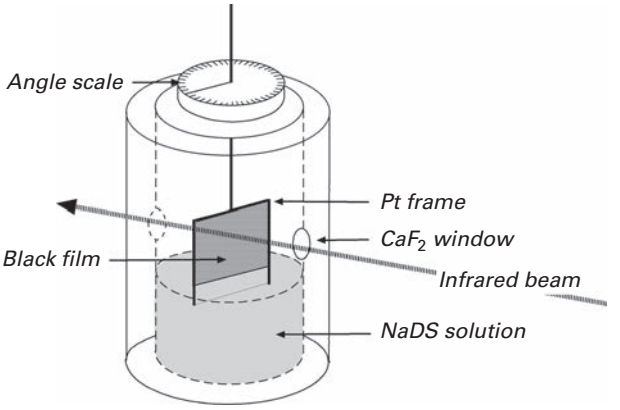

Fig. 3.16 FTIR cell designed for the measurements of vertical black foam films. From ref (44).

surfactants in the presence of chloride ions. In this case it was suggested that the negative charge was acquired by the ion binding of the anions to the head groups (42).

At a critical surfactant concentration which corresponded to about 0.1 CMC, black spots first appear in the film (as indicated by C_b in Fig. 3.15). This leads to the formation of thinner stable black films causing the foam system to become extremely stable. This concentration also corresponds to a relatively high surfactant adsorption density for both surfactant systems. It was found that during this step the onset of charge reduction and high surfactant packing densities occur, which indicates that the state or transition in the single surface monolayer determines the stability of the film.

3.8 The physical chemistry of black films

Foam films have been intensely studied by a range of techniques such as reflectometry, ellipsometry, infrared light and small-angle neutron scattering (SANS) (43). The water content of black films has been quantified by passing an IR beam through a vertical film suspended in a cylindrical tube, which acts as a frame, as shown in Fig. 3.16. The refractive index and the thickness of the surfactant layers and core were determined, as was the OH stretching frequency of the water molecules (44). From FTIR, structural information of the films such as the phases, the orientation of the hydrocarbon chain could be obtained.

Molecular dynamic studies of NBFs prepared from sodium lauryl sulfate indicate 4–6 molecules of water per surfactant molecule (45), which confirms earlier X-ray work (46). Most of the evidence indicates that black films are stabilized by bi-layers of anisotropic chemical surfactant molecules. The structures are elongated and arranged in equidistant rows producing a mesomorphous state (liquid crystalline). The thinnest of the black films (the Newton black film) has a thickness of about 4 nm or about the thickness of a surfactant bilayer. The close-range hydration forces (as introduced in Equation 3.8) have been interpreted in terms of water polarization or reorientation of the confined region and steric forces arising from the thermal fluctuations of the interface.

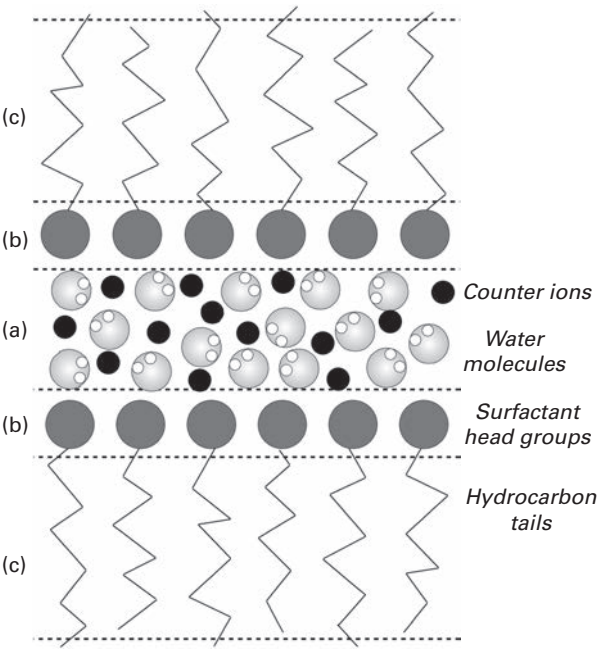

Fig. 3.17 Schematic diagram showing, in profile, the structure of a Newton black film. The diagram contains distinct regions of (a) water molecules and counter ions, (b) chain headgroups and (c) hydrocarbon tails.

SANS has proved to be a valuable tool to probe thin films in bubble structures. A narrow beam of neutrons is reflected on the surface of foams stabilized by deuterated (heavy) fatty acids and collected by a neutron detector. Neutron reflectometry has enabled the composition profile perpendicular to an interface to be investigated, and this has enabled the packing density and layer thickness of the surfactant molecules at the water interface to be studied. SANS studies on foams and thin films stabilized by SDS enabled accurate data on film thickness and bubble size to be recorded (43). Also, interfacial experiments using SANS, neutron scattering and neutron refractivity, together with studies within foams, enabled the multilayered film structure of nonionic polyglycerol ester to be investigated. In order to mimic a coalescence event, the film was compressed to ~ 20% and it was found that the molecular ordering was substantially increased (47). In light of these findings, the structure of an NBF can be summarized as a thin layer (3 to 4 molecules depth) of water molecules and counterion sandwiched in between a surfactant bilayer, as illustrated in Fig. 3.17.

3.9 Rupture mechanism of free microscopic horizontal foam films

As discussed earlier in this chapter, foam films are fragile and may rupture after draining to a critical thickness (h_{cr}), and several theories have been proposed to account for the

rupture process. Early basic studies attributed this rupture to the onset of a thermodynamically unstable state caused by a squeezing action during the thinning process. Significant advancements in understanding the rupture mechanism were made by assuming that thermal and mechanical disturbances are wave-like in nature, causing thickness fluctuations in thin films which lead to either rupture or bubble coalescence at a critical thickness (48). From early theoretical analysis of the hydrodynamic interfacial force balance, the critical thickeners of rupture could be expressed in terms of the attractive van der Waals interactions (characterized by the Hamaker constant), the surface tension and the disjoining pressure. The critical wavelength, λ_{cr}, for the perturbation to grow, assuming the disjoining pressure just exceeds the capillary pressure, has been determined. Film collapse usually occurs when the amplitude of the fast-growing perturbation was equal to the thickness of the film (49), and the critical thickness of rupture, h_{cr}, was defined by the following relationship:

$$h_{cr} = 0.267(a_f A_H{}^2/6\pi\gamma\Delta P)^{1/7} \tag{3.9}$$

where A_H is the Hamaker constant, ΔP is the excess pressure in the film, γ is the surface or interfacial tension and a_f is the initial area of the film. Several modifications have been made to this early equation and these have been discussed in some detail in a review by Manev and Nguyen (28).

However, several discrepancies in the theory have been reported with Maldarelli and Jain (50) having critically reviewed the area of film breaking. It is also well known that many poorly foaming liquids with thick film lamellae are easily ruptured. In fact, pure water films with thicknesses between 110 and 453 nm and ethanol films of thickness of 110 nm appear to break easily (51). Alternative explanation for rupture of relatively thick aqueous films containing low levels of surfactant has involved long-range hydrophobic attractive forces between the surfaces, although more recent studies suggested that rupture can be caused by the spontaneous nucleation of bubbles (forming gas cavities) in the stretched liquid lamella (52, 53, 54).

3.10 Rupture of films between bubbles under dynamic conditions

Cell opening (coalescence) in real foams occurring under extremely dynamic conditions can be defined in terms of deformations, disturbances and surface non-homogeneities. Although this process is extremely difficult to measure or model, it is important from a practical viewpoint to have an estimate of h_{cr} and the coalescence time. Although the magnitude of the drainage rate and critical rupture thickness of single microscopic films under equilibrium and static experimental conditions (isolated from external disturbances) has been established to be less than 100 nm, this is not the situation for thinning films between bubbles under high Reynolds numbers. However, there is considerable evidence in the literature that suggests that h_{cr} values in real foam systems are much higher than the values estimated from thin film drainage experiments. For example, experimental studies on closed polyurethane foam by Zhang and coworker (55) reported

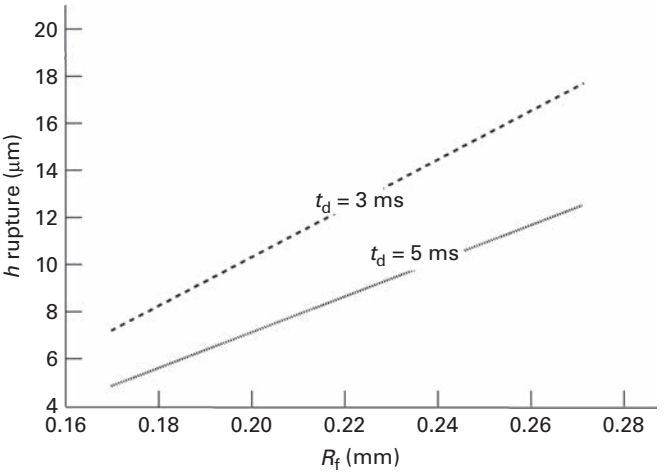

Fig. 3.18 The relationship between the critical rupture thickness (h_{cr}) and film size (R_f) calculated according to the MTR model (29) using experimental data obtained by coalescing bubbles. From ref (57).

a minimum wall rupture thickness of 3500 Å (measured by light interference microscopy), and Neff (56) reported a value critical thickness of 2000 Å for the same foam material which was estimated from the geometry of the Plateau borders.

Recently, Zawala and Malysa (57) carried out coalescence studies of a single bubble at the air/water interface by using a high-speed CCD camera and measured the coalescence time. On approaching and striking the interface, the bubble was observed to rebound and the bubble velocity was rapidly reduced. The bouncing process, impact velocity, size of the film and the coalescence time (the time from the moment of the first bubble collision to rupture) were accurately determined and it was found that that the prolongation of the coalescence process was dependent on the size of the liquid film formed during the bubble collision. In this study, the MTR model was applied using experimentally determined values of the time of film drainage (t_d = 3 and 5 ms) and assuming that the time of film drainage t_d was equal to the time of bubble interaction (contact) with the water/air interface. Using this approach, for an initial film thickness h_i = 0.1 mm, the thickness of rupture was calculated for different size films using Equation (3.3), and the results are shown in Fig. 3.18.

From this figure, critical film thicknesses of 5–12 microns are predicted for the dynamic rupture process between two bubbles – which appear reasonable – and these values are much higher than that of 100 nm for microscopic horizontal films under static conditions. This approach also showed a direct relationship between the increase in critical rupture thickness and increase in film radius – which is in general agreement with the MTR model.

3.11 Importance of fundamental studies on foam films

Common thin films and black films are of great interest because their thicknesses and stability are governed by the same fundamental intermolecular forces as foams,

namely mainly the electrostatic repulsion and van der Waals attraction between surfactant layers. Foam films have also been shown to be capable of detecting pre-micellar surfactant species and surfactant self-assembles and can be used to study the relationship between micellization, adsorption and film hydrodynamics. They have been shown to be useful for studying foam dynamics and drainage, although there are many problems yet to be solved. Studies on foam films have also been of considerable interest to specialists in mineral processing and have enabled a fundamental understanding of the froth flotation of mineral particles to be established (58). Flotation is based on the selective wetting of particles, with different degrees of hydrophobicity, by the thin film and this leads to the attachment of the more valuable particles to the bubble interface. It has also been shown that finely divided particles can also act as foam stabilizers or de-stabilizers depending on the degree of wetting by the solution, and this will be discussed in the later part of this book. In the final stage of flotation, the bubble rises to the surface, carrying the particles which remains weakly attached to the foam layer, where they can be easily removed following rupture of the thin films and break-down of the froth. The drainage rates, critical thickness of rupture and the rupture time of films are important in these selective wetting processes.

Fundamental studies on thin films have had an important impact on our understanding of the behavior of the microscopic membranes that surround every cell in the body. In fact, cell membranes show similar features to thin soap films which make up bubbles. The same experimental techniques traditionally developed to unravel the use of surfactant in bubbles and foams can also be used to understand the functional mechanism of membranes. Cell membranes consisting of lipid bilayers, in which embedded proteins carry out important functions for the cell and can be visualized as fluid-like flat sheets that form a barrier across a cell of living organisms and viruses. The function of the lipid bilayer is to act as a barrier to control the diffusion of ions and proteins into and out of the cell, and it does so by containing almost no water in its core, allowing it to exclude water-soluble salts and sugars diffusing through the cell wall. Thin film studies on phospholipid–protein mixtures and lung surfactants have been applied as models and have been shown capable of detecting the structure, stability and lateral movement of surfactant layers on biological lung membrane systems. (59).

References

(1) H. Nakajima, Two Kinds of Modifications Theories of Light; Some New Observations on the Newton-Hooke Controversy of 1672 Concerning the Nature of Light, *Ann. Sci.*, **41** (3), 261–278, 1984.
(2) *Isaac Newton`s Papers and Letters on Natural Philosophy and Related Documents*, 2nd edn, Ed. I. Bernard Cohen, Harvard University Press, Cambridge, MA, 1978.
(3) J. A. F. Plateau, *Statique Experimentale et Theorique des Liquids Soumis aux Seules Forces Moleculaires*, Vol. **2**, Gauthier-Villars, Paris, 1873.

(4) C. V. Boyle, *Soap Bubbles and the Forces which Mould Them, Reprinted in the Science Study Series*, Heinemann, London, 1960.
(5) R. Young, *Fizzics. The Science of Bubbles, Droplets and Foams*, The John Hopkins University Press, Baltimore, MD, 2011.
(6) S. Perkowitz, *The Universal Foam; The Story of Bubbles from Cappuccino to the Cosmos*, Random House, New York, 2000.
(7a) F. Seychelles, Y. Amarouchene, M. Bessafi and H. Kellay, Thermal Convection and Emergence of Isolated Vortices in Soap Bubbles, *Phys. Rev. Lett.*, **100**, 144501–144505, 2008; (7b) S. Battersby, Soap Bubbles Recreate Jupiter's Turbulent Storms, *New Scientist, Space*, April 10, 2008, www.telegraph.co.uk/science/science-news/10558231/Soap-bubbles-can-predict.
(8) A. Scheludko, Thin Liquid Films, *Adv. Colloid lnterface Sci*., **1**, 391–464, 1967.
(9) A. Scheludko, *Colloid Science*, Elsevier, New York, 1966.
(10) E. Manev, A. Scheludko and D. Exerowa, Effect of Surfactant on the Critical Thickness of Liquid Films, *Colloid. Polym. Sci.*, **252**, 586–593, 1974.
(11) D. Exerowa and P. M. Kruglyakov, *Foam and Foam Films; Theory, Experiment and Application, Studies in Interfacial Sci*, Vol. **5**, Elsevier Publications, 1997.
(12) L. G. C. Pereira, C. Johansson, H. W. Blanch and C. J. Radke, A Bike-Wheel Microcell for Measurement of Thin Film Forces, *Colloids Surf., A*, **186**, 103–111, 2001.
(13) L. G. Cascao-Periera, C. Johansson, C. J. Radke and H. W. Blanch, Surface Forces and Drainage Kinetics of Protein-Stabilized Aqueous Films, *Langmuir*, **19** (18), 7503–7513, 2003.
(14) G. Sethumadhavan, A. D. Nikolov and D. T. Wasan, Stability of Liquid Films Containing Mondispersed Colloidal Particles, *J. Colloid Interface Sci.*, **240**, 105–112, 2001.
(15) A. V. Nguyen, Stefan-Reynolds Equations; Historic Note on the Stefan-Reynolds, *J. Colloid Interface Sci*., **23**(1), 195, 2000.
(16) D. J. Platikanov, Experimental Investigation on the "Dimpling" of Thin Liquid Films, *J. Phys. Chem*., **68**, 3619–3624, 1964.
(17) B. P. Radoev, A. Scheludko and E. Manev, Critical Thickness of Thin Liquid Films: Theory and Experiment, *J. Colloid Interface Sci*., **95**, 254–265, 1983.
(18) S. P. Frankel and K. J. Mysels, Simplified Theory of Reflectometric Thickness Measurements of Structured Soap and Related Films, *J. Appl. Phys.*, **37**, 3725–3728, 1966; K. Mysels, K. S. Frankel and K. Shinoda, *Soap Films*, Pergamon Press, New York, 1959.
(19) Chemical Physics of Colloid Systems and Interfaces. In *Handbook of Surface and Colloid Chemistry*, 3rd edn, Ed. K. S. Birdi, CRC Press, Boca Raton, FL, p. 275.
(20) J. L. Joyce, G. J. Hirasaki and C. A. Miller, Dimple Formation and Behaviour during Axisymmetrical Foam Film Drainage, *Langmuir*, **8**, 3083–3092, 1992.
(21) J. L. Joyce, G. J. Hirasaki and C. A. Miller, Axisymmetrical Drainage of Foam Film Drainage, *Langmuir*, **10**, 3174–3179, 1992.
(22) A. K. Malholtra and D. T. Wasan, Effect of Film Size on Drainage of Foam and Emulsion Films, *A.I.Ch.E. J*, **33**, 1533–1541, 1987.
(23) A. D. Barber and S. Hartland, The Effect of Surface Viscosity on the Axisymmetric Drainage of Planar Liquid Films, *Can. J. Chem. Eng*. **54**, 279–284, 1976.

(24) I. B. Ivanov, *Thin Films, Surfactant Science Series*, Vol. **29**, Marcel Dekker, New York, 1988.
(25) D. C. Tambe and M. M. Sharma, Hydrodynamics of Thin Films Bounded by Viscoelastic Interfaces, *J. Colloid Interface Sci*., **147**, 137–151, 1991.
(26) A. Sharma and E. Ruckenstein, Critical Thickness and Lifetime of Foams and Emulsions; Role of Surface Wave-Inducing Thinning, *J. Colloid Interface Sci.*, **119**, 14, 1987.
(27) D. Valkovska, K. D. Danov and I. B. Ivanov, Stability of Draining Plane-Parallel Films Containing Surfactants, *Adv. Colloid Interface Sci*., **96**, 101–129, 2002.
(28) E. D. Manev and A. V. Nguyen, Critical Thickness of Rupture of Microscopic Thin Liquid Films, *Adv. Colloid Interface Sci*., **114**–115, 133–146, 2005.
(29) E. D. Manev, R. Tsekov and R. J. Radoev, Effect of Thickness Homogeneity on the Kinetic Behavior of Microscopic of Microscopic Foam Film, Experimental and Theoretical, *J. Dispersion Sci. Tech*, **18**, 769–788, 1997.
(30) H. N. Stein, On Marginal Regeneration, *Adv. Colloid Interface Sci.*, **34**, 175–190, 1991.
(31) J. B. N. Hudales and H. N. Stein, Marginal Regeneration of Mobile Vertical Free Liquid Films, *J. Colloid Interface Sci.*, **138**, 354–364, 1990.
(32) P. J. M. Baets and H. N. Stein, Influence of Surfactant Type and Concentration on Drainage of Liquid Films, *Langmuir*, **8**, 3099–3101, 1992.
(33) S. Naire, R. J. Braun and S. A. Snow, Limiting Case of Gravitational Drainage of a Vertical Free Film for Evaluating Surfactants, *J. Soc. Ind. Appl. Math.*, **61** (3), 889–913, 2000.
(34) R. J. Braun, S. A. Snow and S. Naire, Models for Gravitationally – Driven Free – Film Drainage, *J. Eng. Math.*, **43**, 281–314, 2002.
(35) S. Berg, E. A. Adelizzi and S. M. Troian, Experimental Studies of Entrainment and Drainage Flows in Microscopic Soap Films, *Langmuir*, **21**, 3867–3876, 2005.
(36) V. Bergeron, Disjoining Pressure and Film Stability of Alkyltrimethylammonium Bromide Foam Films, *Langmuir*, **13**, 3474–3482, 1997.
(37) B. Derjaguin and Titievskaya, Static and Kinetic Equilibrium of Free Films and Froths. In (Ed.), *Proc. 2nd Int. Congress Surface Activity*, Vol. **1**, Ed. J. H. Schulman, Butterworth, Oxford, UK, p. 211, 1957.
(38) E. J. N. Verwey and J. T. G. Overbeek, *Theory of Stability of Lyophobic Colloids*, Elsevier, Amsterdam, 1948.
(39) K. P. Velikov, O. D. Velev K. G. Marinova and G. N. Constantinides, Effect of the Surfactant Concentration on the Kinetics Stability of Thin Foam and Emulsion Films, *J. Chem. Soc. Faraday Trans.*, **93** (11), 2069–2075, 1997.
(40) A. J. De Vries, Foam Stability, *Rubber Chem. Technol*., **31** (50), 1142–1205, 1958.
(41) E. D. Manev and R. J. Pugh, *Langmuir*, **7**, 2253, 1991; E. D. Manev and R. J. Pugh, *Colloids Surf*., **70**, 289, 1993.
(42) R. Buscall, R. B. Donaldson, R. H. Ottewill and D. Segat, Equilibrium Properties of Foam Films Formed from Nonionic Surface Active Agents. In *Foams*, Ed. R. J. Akers, Chapter 6, pp. 73–88, Academic Press, New York 1976.
(43) M. A. V. Axelos and F. Boue, Foams as Viewed by SANS, *Langmiur*, **19** (17), 6598–6604, 2009.
(44) J. Umemura, M. Matsumoto, T. Kawai and T. Takenaka, Fourier Transform Infrared Studies of Black Foam Films, *Can. J. Chem.*, **67** (7), 1713, 1985.

(45) Z. Gamba, J. Hautman and M. L. Shelley Klein, Molecular Dynamics Investigations of a Newtonian Black Film, *Langmuir*, **8**, 3155–3160, 1992.
(46) A. Belorgey and J. Benattar, Structural Properties of Soap Black Films Investigated by X Ray Reflectivity, *Phys. Rev. Lett.*, **66**, 313–316, 1991.
(47) C. Curschellas and Coworkers, Foams Stabilized by Multi-lamellar Polyglycerol Ester Self Assemblies, *Langmuir*, **29** (1), 38– 2013.
(48) A. J. De Vries, Possible Mechanism for the Spontaneous Rupture of Thin Free Liquid Films, *Disc. Faraday Soc*., **42**, 23–33, 1966.
(49) A. Vrij and T. J. Overbeek, Rupture of Thin Liquid Films Due to Spontaneous Fluctuations in Thickness, *J. Am. Chem. Soc.*, **90**, 3074–3078, 1968.
(50) C. Maldarelli and R. K. Jain. In *Thin Liquid Films*, Ed. I. B. Ivanov, Dekker, New York, 1988.
(51) L. Doubliez, The Drainage and Rupture of Non-Foaming Liquid Film Formed upon Impact with a Free Surface, *Int. J. Multiphase Flow*, **17** (6), 783–803, 1991.
(52) R. J. Pugh and R. Yoon, Hydrophobic Forces in Thin Aqueous Films, *J. Colloid Interface Sci*., **163**, 169–176, 1994.
(53) J. K. Angarska and Coworker, Detection of Hydrophobic Surface Forces in Foam Films by Measurement of the Critical Thickness of Ruptures, *Langmuir*, **20** (5), 1709–1006, 2004.
(54) S. I. Karakashev and A. V. Nguyen, Do Liquid Films Rupture Due to the So-called Hydrophobic Force or Migration of Dissolved Gas, *Langmuir*, **25** (6), 3363–3368, 2009.
(55) X. D. Zhang, H. T. Davis and C. W. Macosko, *J. Cell. Plastics*., **35**, 458, 1999.
(56) R. A. Neff, *Reactive Processing of Flexible Polyurethane Foam*, Dept of Chemical Eng., University of Minneapolis Press, Minnesota, 1995.
(57) J. Zawala and K. Malysa, Influence of Impact Velocity and Size of the Film Formed on Bubble Coalescence Time at Water Surface, *Langmuir*, **27**, 2250–2257, 2011.
(58) R. J. Pugh, The Study of Thin Aqueous Films as Models for Froths and Flotation. In *Innovations in Flotation Technology*, P. Mavros and K. A. Matis, Eds., Kluwer, Netherlands, pp. 1–24, 1992.
(59) D. Platikanov and D. Exerowa, Thin Liquid Films and Foams; Classic and Modern Topics, *Curr. Opin. Colloid Interface Sci*., **13**, 97–99, 2008.